Atmos. Chem. Phys. Discuss., doi:10.5194/acp-2016-981, 2016
Manuscript under review for journal Atmos. Chem. Phys.
Published: 29 November 2016

Atmospheric Chemistry and Physics Discussions

WRF-Chem simulation of aerosol seasonal variability in the San Joaquin Valley

Longtao Wu[1], Hui Su[1], Olga V. Kalashnikova[1], Jonathan H. Jiang[1], Chun Zhao[2], Michael J. Garay[1], James R. Campbell[3] and Nanpeng Yu[4]

1. Jet Propulsion Laboratory, California Institute of Technology, Pasadena, CA, USA

2. Atmospheric Sciences and Global Change Division, Pacific Northwest National Laboratory, Richland, WA, USA

3. Naval Research Laboratory, Monterey, CA, USA

4. University of California, Riverside, Riverside, CA, USA

Submitted to *Atmospheric Chemistry and Physics*

November, 2016

Corresponding author address: Longtao Wu, 4800 Oak Grove Dr., Pasadena, CA 91109
E-mail: Longtao.Wu@jpl.nasa.gov

Atmos. Chem. Phys. Discuss., doi:10.5194/acp-2016-981, 2016
Manuscript under review for journal Atmos. Chem. Phys.
Published: 29 November 2016

Atmospheric Chemistry and Physics Discussions

Highlights:

1. The WRF-Chem simulation successfully captures aerosol variations in cold season in the San Joaquin Valley (SJV), but has poor performance in warm season.
2. High resolution model simulation can better resolve inhomogeneous distribution of anthropogenic emissions in urban areas, resulting in better simulation of aerosols in cold season in the SJV.
3. Observations show that dust is a major component of aerosols in the SJV, especially in warm season. Poor performance of the WRF-Chem model in warm season in the SJV is mainly due to misrepresentation of dust emission and vertical mixing.

Atmos. Chem. Phys. Discuss., doi:10.5194/acp-2016-981, 2016
Manuscript under review for journal Atmos. Chem. Phys.
Published: 29 November 2016

Abstract

WRF-Chem simulations of aerosol seasonal variability in the San Joaquin Valley (SJV), California are evaluated by satellite and in-situ observations. Results show that the WRF-Chem model successfully captures the distribution, magnitude and variation of SJV aerosols in cold season. However, the aerosols are not well represented in warm season. Aerosol simulations in urban areas during the cold season are sensitive to model horizontal resolution, with better simulations at 4 km resolution than at 20 km resolution, mainly due to inhomogeneous distribution of anthropogenic emissions. In rural areas, the model sensitivity to grid size is rather small. Our observational analysis show that dust is a primary contributor to aerosols in the SJV, especially in the warm season. Aerosol simulations in the warm season are sensitive to parameterization of dust emission in the WRF-Chem model. The GOCART (Goddard Global Ozone Chemistry Aerosol Radiation and Transport) dust scheme produces very little dust in the SJV while the DUSTRAN (DUST TRANsport model) scheme overestimates dust emission. Vertical mixing of aerosols is not adequately represented in the model comparing to CALIPSO (Cloud-Aerosol Lidar and Infrared pathfinder Satellite Observation) aerosol extinction profiles. Improved representation of dust emission and vertical mixing are needed for better simulations of aerosols in warm season in the SJV. Aerosols generated by wild fires are not captured in the simulations with climatological fire emissions, underscoring the need of fire emission observations for operational usage.

Atmos. Chem. Phys. Discuss., doi:10.5194/acp-2016-981, 2016
Manuscript under review for journal Atmos. Chem. Phys.
Published: 29 November 2016

1. Introduction

The San Joaquin Valley (SJV) in the southern portion of the California Central Valley is surrounded by coastal mountain range to the west and the Sierra Nevada range to the east. With cool wet winters and hot dry summers, the unique natural environment makes SJV one of the most productive agricultural regions in the world (SJV APCD, 2012 and references therein). However, SJV is also one of the most polluted regions in US due to its unique geographical location. Frequent stagnant weather systems are conducive to air pollution formation while the surrounding mountains block air flow and trap pollutions. Large seasonal and spatial variations of aerosols are observed in the SJV. Although significant progress at improving local air quality in past decades has been made through strong emission controls, the PM2.5 (particulate matter with diameter ≤ 2.5 μm) concentrations in the SJV remain well above the national ambient air quality standards (NAAQS) threshold of 12 μg m^{-3} on annual basis and 35 μg m^{-3} on daily basis, mainly during cold season. Improved understanding of the aerosol variabilities and their impact are needed to provide further guidance for emission control strategies in the SJV.

Air quality models are a critical tool to understand the formation and evolution of aerosols and their impacts on air quality and climate. However, it is still quite a challenge to accurately simulate aerosol properties (Fast et al., 2014). Fast et al. (2014) summarized the factors contributing to the errors in region-scale modeling of aerosol properties, including 1) emission sources; 2) meteorological parameterizations; 3) representation of aerosol chemistry; 4) limited understanding of the formation processes of secondary organic aerosol (SOA); 5) spatial resolution; and 6) boundary conditions.

As one of the advanced regional air quality models, the Weather Research and Forecasting model with Chemistry (WRF-Chem) has been widely used to study aerosols and

Atmos. Chem. Phys. Discuss., doi:10.5194/acp-2016-981, 2016
Manuscript under review for journal Atmos. Chem. Phys.
Published: 29 November 2016

their impacts on regional air quality and climate (e.g., Misenis and Zhang, 2010; Zhang et al., 2010; Zhao et al., 2010; 2013; 2014; Wu et al., 2011a, 2011b, 2013; Fast et al., 2012, 2014; Scarino et al., 2014; Tessum et al., 2015; Campbell et al., 2016; Hu et al., 2016). Fast et al. (2014) showed that WRF-Chem simulations at 4 km horizontal resolution captured the observed meteorology and boundary layer structure over California in May and June of 2010. The model reasonably simulated the spatial and temporal variation of aerosols. Aerosol simulations by WRF-Chem are usually sensitive to both local emission and long-range transport of aerosols from the boundary conditions provided by the global Model for Ozone and Related chemical Tracers, version 4 (MOZART-4). Similarly, in a one-year simulation at 12 km horizontal resolution, Zhao et al. (2013) showed that the WRF-Chem model represented the observed seasonal and spatial variation of surface particulate matter (PM) concentration over California. However, underestimation of elemental carbon (EC) and organic matter were noticed in the model simulation, with no sensitivity to horizontal model resolution.

In this study, we extend the studies by Fast et al. (2014) and Zhao et al. (2013) by focusing on simulating aerosol seasonal variability in the most polluted SJV in California. This paper serves as the first step for future investigation of the aerosol impact on regional climate and the water cycle in California. Previous studies have demonstrated that aerosols are better simulated at higher model resolution (Misenis and Zhang et al., 2010; Qian et al., 2010; Stround et al., 2011; Fountoukis et al., 2013). However, most regional climate studies are still limited to coarse model resolutions (on the order of 10 km) due to the availability of computational resources. This study will investigate the sensitivity of aerosol simulations to horizontal resolution and identify suitable model resolution for regional climate study in the SJV.

Atmos. Chem. Phys. Discuss., doi:10.5194/acp-2016-981, 2016
Manuscript under review for journal Atmos. Chem. Phys.
Published: 29 November 2016

92 Another application of air quality modeling is to provide initial *a priori* input for remote
93 sensing retrievals. The WRF-Chem model has been proposed as an input for retrieval algorithms
94 to be developed for the recently-selected NASA (National Aeronautics and Space
95 Administration) MAIA (Multi-Angle Imager for Aerosols) mission, which aims to map PM
96 component concentrations in major urban areas (including the SJV). A reasonable initial estimate
97 of aerosol speciation from WRF-Chem is critical to ensure the retrieval speed and quality.
98 Considering the sensitivity of WRF-Chem simulations to various factors such as initial and
99 boundary conditions, model parameterizations and emission sources (e.g., Wu and Petty, 2010;
100 Zhao et al., 2010, 2013; Wu et al., 2011a, 2015; Fast et al., 2014; Campbell et al., 2016;
101 Morabito et al., 2016), careful model evaluations are needed before the simulations can be used
102 for remote sensing retrievals. This study also serves as an evaluation for WRF-Chem aerosol
103 simulations in the SJV, which will provide important information for utilizing WRF-Chem for
104 MAIA retrieval algorithms, critical to the success of the MAIA mission.
105 This paper is organized as follows. Section 2 describes observational datasets used for
106 model evaluation. Section 3 provides the description of the WRF-Chem model and experiment
107 setup. Model simulations and their comparison with observations are discussed in section 4.
108 Section 5 presents the conclusions.

109 ## 2. Observations

110 ### 2.1 Aerosol Optical Depth

111 Aerosol optical depth (AOD) is a measure of column-integrated light extinction by
112 aerosols and a proxy for total aerosol loading in the atmospheric column. The Aerosol Robotic
113 Network (AERONET) provides ground measurements of AOD every 15 minutes during daytime
114 (Holben et al., 1998), with an accuracy of ±0.01 (Eck et al., 1999; Holben et al., 2001). The

Atmos. Chem. Phys. Discuss., doi:10.5194/acp-2016-981, 2016
Manuscript under review for journal Atmos. Chem. Phys.
Published: 29 November 2016

115 monthly level 2.0 product with cloud screening and quality control is used in this study.
116 AERONET AOD is interpolated to 0.55μm using the Ångström exponent. In the SJV, only one
117 AERONET station at Fresno, CA has regular observations throughout the California water year
118 2013 (WY2013; i.e., from October 2012 to September 2013).

119 The Multiangle Imaging Spectroradiometer (MISR) (Diner et al., 1998) instrument
120 onboard the Terra satellite has provided global coverage of AOD once a week since December
121 1999. The standard MISR retrieval algorithm provides AOD observations at 17.6 km resolution
122 using 16 x 16 pixels of 1.1 km each. About 70% of MISR AOD retrievals are within 20% of the
123 paired AERONET AOD, and about 50% of MISR AOD falls within 10% of the AERONET
124 AOD, except in the dusty and hybrid (smoke+dust) sites (Kahn et al., 2010). We use version 22
125 of Level 3 monthly AOD product at 0.5° resolution in this study.

126 **2.2 Surface Mass Concentration**

127 Surface PM2.5 speciation and PM10 (particulate matter with diameter ≤ 10 μm) data are
128 routinely collected by two national chemical speciation monitoring networks: Interagency
129 Monitoring of Protected Visual Environments (IMPROVE) and the PM2.5 National Chemical
130 Speciation Network (CSN) operated by Environmental Protection Agency (EPA) (Hand et al.
131 2011; Solomon et al., 2014). IMPROVE collects 24-h aerosol speciation every third day at
132 mostly rural sites since 1988. The same frequency of aerosol speciation data was collected at
133 EPA CSN sites in urban and suburban areas since 2000. Selected IMPROVE and EPA CSN sites
134 used in this study are shown in Figure 1a.

135 **2.3 Aerosol Extinction Profile**

136 The aerosol extinction coefficient profile reflects the attenuation of the light passing
137 through the atmosphere due to the scattering and absorption by aerosol particles as a function of

Atmos. Chem. Phys. Discuss., doi:10.5194/acp-2016-981, 2016
Manuscript under review for journal Atmos. Chem. Phys.
Published: 29 November 2016

range. Version 3 Level 2 532 nm aerosol extinction profiles derived from Cloud-Aerosol Lidar with Orthogonal Polarization (CALIOP) backscatter profiles collected onboard the Cloud-Aerosol Lidar and Infrared pathfinder Satellite Observation (CALIPSO) satellite are used (Omar et al., 2009; Young and Vaughan, 2009). Seasonal mean profiles are derived for WY2013 based on the methodology outlined in Campbell et al. (2012), whereby quality-assurance protocols are applied to individual profiles before aggregating and averaging the data. We highlight that no individual profiles are included in the averages if the CALIOP Level 2 retrieval failed to resolve any extinction within the column, a potential biasing issue that has recently been described by Toth et al. (2016). Level 2 532 nm aerosol extinction is speciated, with algorithms resolving aerosol type present for clean marine, dust, polluted continental, clean continental, polluted dust and smoke. Dust and polluted dust are specifically distinguished in the averages applied below for their contribution to total extinction and the vertical profile seasonally in the SJV.

2.4 Equivalent Potential Temperature

Equivalent potential temperature (θ_e) is a quantity relevant to the stability of the air. The θ_e profiles used in this study are derived from temperature and moisture profiles observed by AIRS (Atmospheric Infrared Sounder) onboard the Aqua satellite (Susskind et al., 2003; Divakarla et al., 2006). AIRS has provided global coverage of the tropospheric atmosphere at approximately 01:30 and 13:30 local time since 2002. AIRS retrievals have root-mean-squared (RMS) difference of ~1 K for temperature and ~15% for water vapor (Divakarla et al., 2006). Level 3 monthly temperature and moisture retrievals (version 6) at 1° x 1° grid are used in this study.

3. Model Description and Experiment Setup

The WRF-Chem model Version 3.5.1 (Grell et al., 2005) updated by Pacific Northwest National Laboratory (PNNL) is used in this study (Zhao et al., 2014). Similar to the chemical

Atmos. Chem. Phys. Discuss., doi:10.5194/acp-2016-981, 2016
Manuscript under review for journal Atmos. Chem. Phys.
Published: 29 November 2016

parameterizations used in the Zhao et al. (2014), this study uses the CBM-Z (carbon bond mechanism) photochemical mechanism coupled with the four-sectional-bin MOSAIC (Model for Simulating Aerosol Interactions and Chemistry) aerosol scheme as the chemical driver. The major components of aerosols (nitrate, ammonium, EC, organic carbon, sulfate, sea salt, dust, etc.) as well as their physical and chemical processes are simulated in the model. More details of the chemical settings used in this study can be found in Zhao et al. (2014) and references therein.

The model simulations start on 1 September 2012 and run continuously for 13 months. With the first month as spin-up, our analysis focuses on WY2013 from October 2012 to September 2013.The model is configured with 40 vertical levels and a model top at 50 hPa. The model center is placed at 38°N, 121°W, with 250 x 350 grids at 4 km horizontal resolution (referred to as "4km" hereafter; Table 1), covering California and the surrounding area. To test the sensitivity of aerosol simulations on horizontal resolution, one simulation with the same model settings and domain coverage is conducted at 20 km horizontal resolution (referred to as "20km" hereafter).

The physics parameterizations used in the simulations include the Morrison double-moment microphysics scheme (Morrison et al., 2009), Rapid Radiative Transfer Model for General circulation model (RRTMG) shortwave and longwave radiation schemes (Iacono et al., 2008), Yonsei University (YSU) planetary boundary layer scheme (Hong et al., 2006), Community Land Model (CLM) Version 4 land surface scheme (Lawrence et al., 2011). Grell 3D ensemble cumulus scheme (Grell and Devenyi, 2002) is used in the 20km simulation while the 4km simulation does not use cumulus parameterization. The ERA-Interim reanalysis data (Dee et al., 2011) provides meteorological initial and boundary conditions for the WRF-Chem. The MOZART-4 global chemical transport model (Emmons et al., 2010) is used for the chemical initial and boundary conditions. Fast et al. (2014) found that the MOZART-4 model has overestimation of aerosols in

Atmos. Chem. Phys. Discuss., doi:10.5194/acp-2016-981, 2016
Manuscript under review for journal Atmos. Chem. Phys.
Published: 29 November 2016

the free troposphere over California. Following Fast et al. (2014), the chemical initial and boundary conditions from MOZART-4 are divided by two in all simulations.

Anthropogenic emissions are provided by US EPA 2005 National Emissions Inventory (NEI05), with area-type emissions on a structured 4-km grid and point type emissions at latitude and longitude locations (US EPA, 2010). Anthropogenic emissions are updated every hour to account for diurnal variability, while its seasonal variation is not considered in the simulations. Biogenic emissions are calculated online using the Model of Emissions of Gases and Aerosols from Nature (MEGAN) model (Guenther et al., 2006). Biomass burning emissions are obtained from the Global Fire Emissions Database, version 2.1 with eight-day temporal resolution (Randerson et al., 2007). Sea salt emissions use the PNNL-updated sea salt emission scheme that includes the correction of particles with radius less than 0.2 μm (Gong et al., 2003) and dependence on sea surface temperature (Jaeglé et al., 2011).

Following Zhao et al. (2013), dust emission is computed from the GOCART (Goddard Global Ozone Chemistry Aerosol Radiation and Transport) dust scheme (Ginoux et al., 2001) in the 20km and 4km simulations. As shown later, a significant amount of dust is observed in the SJV while the GOCART dust scheme produces little dust. One sensitivity experiment at 4 km horizontal resolution (referred to as "4km_D2" hereafter) is conducted by switching dust emission scheme to the DUST TRANsport model (DUSTRAN) scheme (Shaw et al., 2008). Detailed descriptions of the two dust emission schemes can be found in Zhao et al. (2010).

4. Model Simulation Results

WRF-Chem model simulation results and their evaluations are in this section. We start the discussions with a focus on the polluted urban areas. Because aerosols properties and model performance are similar at all urban sites, our discussion is focused on the results at Fresno, CA

Atmos. Chem. Phys. Discuss., doi:10.5194/acp-2016-981, 2016
Manuscript under review for journal Atmos. Chem. Phys.
Published: 29 November 2016

while those at other urban sites are provided in supplementary materials. Model simulations in rural areas are presented in the last subsection.

4.1 Sensitivity to Horizontal Resolution

Figure 1 shows daily mean anthropogenic PM2.5 emission rates used in the 20km and 4km simulations, respectively. Although both of the PM2.5 emission rates are derived from the 4 km NEI05 dataset, localized high emission rates with sharp gradients are evident at urban areas in the 4km simulation (Figure 1b). The 20km simulation has lower emission rates with smoother features due to the averaging process (Figure 1a).

Consistent with the emission rate differences, higher AOD is simulated at 4km than 20km, mainly in cold season (OND and JFM in Figure 2). The 4km simulation reproduces the distribution and magnitude of AOD observed by MISR well in the cold season. The AOD difference between 20km and 4km is small in the warm season (AMJ and JAS in Figure 2). Both the 20km and 4km runs underestimate AOD in the warm season compared with MISR. Model performance identified in Figure 2, including the sensitivity to horizontal resolution in cold season and underestimation of AOD in warm season, are further confirmed by comparing to AERONET observations at Fresno, CA (Figure 3). In cold season at Fresno, the AOD in the 20km simulation is 23% lower than the AOD in the 4km simulation. The different model sensitivities to horizontal resolution from the cold to the warm season suggest that the dominant aerosol sources are different through the two seasons. We will elaborate upon the aerosol composition in the following section. AERONENT shows small seasonal variation of AOD in the SJV, which is not well represented in the 20km and 4km simulations (Figure 2 and 3).

Aside from AOD, significant seasonal variability of PM2.5 is observed in the SJV urban areas (Figure 4a and Supplementary Figure 1a and 2a). PM2.5 at Fresno peaks in January (26.18

Atmos. Chem. Phys. Discuss., doi:10.5194/acp-2016-981, 2016
Manuscript under review for journal Atmos. Chem. Phys.
Published: 29 November 2016

230 μg m^{-3}) and has minimum of 7.03 μg m^{-3} in June, with an annual nonattainment value of 12.64 μg
231 m^{-3} in total (Figure 4a). All WRF-Chem simulations successfully capture the seasonal variability
232 of PM2.5 observed in the SJV.

233 In the cold season, the 4km simulation overestimates PM2.5 by 27% while the 20km
234 simulation exhibits a low bias of 19% compared with IMPROVE observations at Fresno (Table 2).
235 High PM2.5 concentrations are primarily nitrate. Both simulations produce seasonal variability of
236 nitrate, but with high biases of 17% in 20km and 75% in 4km in the cold season (Figure 4c). It
237 suggests that the NEI05 dataset may have a high bias in nitrate emissions, which was also found
238 in Texas (Kim et al., 2011). OC, the second largest contributor of cold season PM2.5 in the SJV,
239 is significantly underestimated by 76% in the 20km simulation (Figure 4f). The 4km simulation
240 produces more OC than the 20km simulation, but it is still lower than IMPROVE by 46%. Fast et
241 al. (2014) suggested that the low bias in the WRF-Chem simulation is primarily due to incomplete
242 understanding of SOA processes.

243 Significant underestimation of EC and sulfate in the cold season are also shown in the
244 20km simulation, while the 4km simulation exhibits good agreement with IMPROVE (Figure 4d
245 and 4e). Sulfate in both simulations exhibits a low bias of ~45% in the warm season. Low bias of
246 simulated sulfate, with a failure of capturing the peaks during late afternoon, was also shown at
247 Bakersfield in Fast et al. (2014). It suggests that improvement in understanding the photochemical
248 processes involving sulfate is needed to reproduce seasonal variability of sulfate in the SJV. The
249 4km simulation of PM10 has good agreement with IMPROVE in winter (December, January and
250 February), but a large low bias is found in other months (Figure 4b). The 20km simulation
251 underestimates PM10 throughout WY2013.

Atmos. Chem. Phys. Discuss., doi:10.5194/acp-2016-981, 2016
Manuscript under review for journal Atmos. Chem. Phys.
Published: 29 November 2016

Overall, the 4km simulation produce higher AOD and surface PM than the 20km simulation in urban areas of the SJV, especially in the cold season. The 4km simulation has better agreement with satellite and surface observations than the 20km simulation. The 4km simulation captures seasonal variability of PM2.5 and its speciation. However, significant underestimation of AOD and PM10 are shown during the warm season in both 4km and 20 km simulations. The underestimation also exists in a sensitivity experiment initialized in April (not shown). The relatively good performance in simulating PM2.5 but PM10 suggests that coarse aerosol particle mass (CM; 10 μm ≥ particulate matter with diameter > 2.5 μm), mainly dust in the SJV, is not represented well in the simulations. The impact of dust parameterizations is investigated in the 4km_D2 experiment.

4.2 Sensitivity to Dust Scheme

Limited amounts of PM2.5_dust (dust with diameter ≤ 2.5 μm) are observed in the SJV cold season, with a minimum in December (Figure 5c). The amount of PM2.5_dust increases in the warm season, with a peak in September. The 4km simulation produces comparable PM2.5_dust to IMPROVE in the winter, but almost no dust in other months. The 4km_D2 simulation represents well the magnitude of PM2.5_dust in cold season. However, too much PM2.5_dust is simulated in warm season, resulting in an overestimation of PM2.5 by 52% (Figure 5b and Table 2). Both the 4km and 4km_D2 simulations capture seasonal variability of PM2.5, but not for PM10 (Figure 5a). The magnitude of PM10 in the 4km_D2 is larger than the 4km simulation. PM10 in the 4km_D2 is overestimated in AMJ but underestimated in JAS, leading to comparable season mean with IMPROVE observations.

On the relative contribution of different aerosol species, IMPROVE observations at Fresno show that nitrate is the primary contributor (32.3%) to PM2.5 while only 5.3% of PM2.5 is dust

Atmos. Chem. Phys. Discuss., doi:10.5194/acp-2016-981, 2016
Manuscript under review for journal Atmos. Chem. Phys.
Published: 29 November 2016

275 in the cold season (panel 1 of Figure 6). Both 4km and 4km_D2 roughly reproduce the relative
276 contributions to PM2.5 in the cold season, with an overestimation of nitrate and underestimation
277 of OC found in Figure 4. Relative contributions of dust to PM2.5 are better simulated in 4km_D2
278 than in 4km. IMPROVE shows that 46.6% of PM10 is in the cold season (panel 2 of Figure 6).
279 Both 4km (6.3%) and 4km_D2 (20.6%) underestimate the contribution of CM to PM10. In the
280 warm season, dust (24.6%) becomes the primary contributor to PM2.5 while the contribution from
281 nitrate decreases to 9.9% as observed by IMPROVE (panel 3 of Figure 6). Almost no PM2.5_dust
282 is simulated in 4km while too much PM2.5_dust is produced in 4km_D2 in the warm season. The
283 relative contribution of CM to PM10 is too small (27.6%) in 4km while 4km_D2 has better relative
284 contribution of 66.3% comparing to IMPROVE observed 75.8% (panel 4 of Figure 6).

285 AOD simulations are improved in the 4km_D2 experiment (Figure 7), with better
286 agreement with MISR (Figure 2). AOD in 4km_D2 is comparable to observations in AMJ, but still
287 underestimated in JAS. Consistent with AOD, the vertical distribution of aerosol extinction is
288 reasonably simulated in cold season in the WRF-Chem simulations while large discrepancies are
289 shown in warm season (Figure 8). As observed by CALIOP at 532 nm, aerosols are mainly
290 confined below 1 km above the surface in the cold season. Model simulations reasonably capture
291 the vertical distribution of aerosol extinction observed by CALIOP, with low biases in the
292 boundary layer and high biases in the free atmosphere. Similar discrepancy between the model
293 simulations and CALIOP is shown in other studies (Wu et al., 2011a; Hu et al., 2016). The
294 difference between 4km and 4km_D2 is small in cold season.

295 Dust in the boundary layer is a primary factor contributing to aerosol extinction in the SJV,
296 as illustrated by the differences between the bulk seasonal CALIOP mean profile and those
297 excluding the contributions of the dust and polluted dust species (CALIOP_nodust) profiles

Atmos. Chem. Phys. Discuss., doi:10.5194/acp-2016-981, 2016
Manuscript under review for journal Atmos. Chem. Phys.
Published: 29 November 2016

(Figure 8). The simulated aerosol extinctions fall between the two in all seasons, suggesting relatively good performance of simulating aerosols except for dust. Although a small portion of PM2.5 is dust in the cold season, dust contributes to about 50% of total aerosol extinction (Figure 8a and 8b). A predominate portion of aerosol extinction in the boundary layer is contributed to by dust in the warm season (Figure 8c and 8d). There, the 4km_D2 simulation produces higher aerosol extinction in the boundary layer than the 4km simulation, though it is still lower than CALIOP.

Overall, poor simulations of dust play the dominant role in the bias of aerosols, especially in warm season. Both the GOCART and DUSTRAN dust emission schemes used in this study have problems in reproducing dust emission in the SJV, with underestimation in GOCART and overestimation in DUSTRAN (Figure 5c). Improvement on dust emission is required for correctly simulating seasonal variability of aerosols in the SJV.

4.3 The Role of Meteorology

In the warm season, more aerosols are observed at higher altitude than during the cold season (Figure 8). A well-mixed layer of aerosols is observed below 1.5 km in AMJ (Figure 8c), consistent with the large instability below 1.5 km observed by AIRS (Figure 9c). Both simulations fail to capture this mixed layer of aerosols (Figure 8c) due to weak vertical mixing as evidenced by relatively small instability in the simulations (Figure 9c). Aerosol extinction gradually decreases with height in the simulations (Figure 8c). Similar biases of aerosol and instability in the boundary layer are also shown in JAS (Figure 8d and 9d). Weak instability in the simulation, which limits vertical mixing of aerosols, likely enhances the low bias of JAS AOD (Figure 7). Although the 4km_D2 experiment produces comparable AOD and surface mass in AMJ (Figure 5 and Figure 7), the vertical distribution of aerosols is not well represented (Figure 8). The comparable AOD in 4km_D2 results from the low bias in the boundary layer and high bias in the free atmosphere. The

Atmos. Chem. Phys. Discuss., doi:10.5194/acp-2016-981, 2016
Manuscript under review for journal Atmos. Chem. Phys.
Published: 29 November 2016

high bias in the free atmosphere suggests that the low bias in AOD are not due to the halved chemical boundary conditions from MOZART-4. The stability biases in cold season are relatively small (Figure 9a and 9b), consistent with good performance of aerosol simulation in the cold season. These results highlight that the vertical mixing of dust must be correctly represented in order to resolve the aerosol extinction profile correctly. Improved simulation of boundary layer physics and dynamics during the warm season in the SJV warrants future investigation.

4.4 Results in Rural Areas

In general, low values of PM concentration are observed in the rural areas, Pinnacles and Kaiser (Figure 10 and 11). The rural areas share some similar model performance with the urban areas, such as the overestimation of nitrate, reasonable simulation of EC, good representation of sulfate in cold season and underestimation of sulfate in warm season. However, the sensitivity to model resolution is not significant. It suggests that high model resolution is particularly important for heavily polluted areas due to the inhomogeneity of emission sources, but less important for relatively lightly polluted areas.

In late July/early August, MODIS (Moderate Resolution Imaging Spectroradiometer) fire data (not shown) observed active wild fires close to Kaiser, which resulted in high concentration of aerosols at Kaiser (Figure 11). Our model simulations with climatological fire emissions fail to reproduce these fire events. Based on fire locations from satellite observations, Wu et al. (2011a) has demonstrated that the WRF-Chem model can capture aerosols distributions from wild fires over South America. Campbell et al. (2016) further described the difficulties in both constraining total aerosol mass from operational satellite fire observations and the time necessary within the model for diffusion within the near-surface layers to render both reasonable AOD and vertical

Atmos. Chem. Phys. Discuss., doi:10.5194/acp-2016-981, 2016
Manuscript under review for journal Atmos. Chem. Phys.
Published: 29 November 2016

profiles of aerosol extinction. For operational application of the WRF-Chem model in MAIA retrievals, the observations of fire events need to be considered.

5. Summary

The WRF-Chem model is applied to simulate seasonal variability of aerosols in WY2013 (water year 2013) in the SJV (San Joaquin Valley). Model simulations are evaluated using satellite and in-situ observations. In general, the model simulations at 4 km resolution reproduce the spatial and temporal variations of aerosols in cold season, when aerosols are mainly contributed by anthropogenic emissions in the SJV. The magnitude of simulated aerosols in the cold season, especially in the urban areas, is sensitive to model horizontal resolution. The 4km simulation has comparable magnitude to the observations while the 20km simulation underestimates aerosols. The differences of aerosol simulations between different model resolutions are mainly due to the difference in aerosol emissions. Emissions at higher resolution can better resolve the inhomogeneity of anthropogenic emissions in the SJV than at lower resolution. The sensitivity to horizontal resolution is small in the rural areas and in warm season, when the contribution of anthropogenic emissions is small.

Previous studies in the SJV are mainly focused on PM2.5 (particulate matter with diameter $\leq$ 2.5 μm) and during cold season (e.g. Chow et al., 2006; Herner et al., 2006; Pun et al., 2009; Ying and Kleeman, 2009; Zhang et al., 2010; Chen et al., 2014; Hasheminassab et al., 2014; Kelly et al., 2014; Baker et al., 2015; Brown et al., 2016). CALIOP (Cloud-Aerosol Lidar with Orthogonal Polarization) and IMPROVE (Interagency Monitoring of Protected Visual Environments) observations show that dust is a primary contributor to aerosols in the SJV in warm season. Dust contributes 24.6% to PM2.5 while more than 75.8% to PM10 (particulate matter with diameter $\leq$ 10 μm) in warm season. For all seasons, the major component of aerosol extinction in

Atmos. Chem. Phys. Discuss., doi:10.5194/acp-2016-981, 2016
Manuscript under review for journal Atmos. Chem. Phys.
Published: 29 November 2016

366 the boundary layer is dust as observed by CALIOP, consistent with Kassianov et al. (2012). For a
367 complete understanding of aerosol impact on air quality and regional climate, the full spectrum of
368 aerosols should be considered during all seasons.

369 All the model simulations fail to capture aerosol distribution and variability in the SJV
370 warm season, largely due to the misrepresentation of dust emission and vertical mixing. The
371 GOCART (Goddard Global Ozone Chemistry Aerosol Radiation and Transport) dust emission
372 scheme significant underestimates dust while the DUSTRAN (DUST TRANsport model) scheme
373 may overestimate dust emission in the SJV. Along with the bias in dust emissions, our simulations
374 produce weak atmospheric instability in warm season, leading to weak vertical mixing. Improved
375 dust emission and better simulations of boundary layer properties are needed for correct simulation
376 of aerosols in warm season in the SJV.

377 Other biases are also identified in the model simulations. Nitrate in the cold season is
378 overestimated in the model, possibly due to the overestimation of emissions. Incomplete
379 understanding of SOA (secondary organic aerosol) could contribute to the underestimation of OC
380 (organic carbon). Underestimation of sulfate in the warm season may be due to incorrect
381 photochemical processes of sulfate in the model. Aerosols from wild fires are not captured in the
382 simulations with climatological fire emissions. Further investigations are needed to improve model
383 simulations in the SJV for both scientific and operational applications. The evaluation framework
384 used in this study can be used to other polluted regions to ensure that aerosols are simulated
385 correctly for the right reasons.

386 ## Acknowledgements

387 The research described in this paper was carried out at the Jet Propulsion Laboratory,
388 California Institute of Technology, under a contract with the National Aeronautics and Space

Atmos. Chem. Phys. Discuss., doi:10.5194/acp-2016-981, 2016
Manuscript under review for journal Atmos. Chem. Phys.
Published: 29 November 2016

Administration. The authors thank the funding support from the NASA ACMAP program and JPL PDF program. This work is partially sponsored by California Energy Commission under grant #EPC-14-064.

References

Baker, K. R., Carlton, A. G., Kleindienst, T. E., Offenberg, J. H., Beaver, M. R., Gentner, D. R., Goldstein, A. H., Hayes, P. L., Jimenez, J. L., Gilman, J. B., de Gouw, J. A., Woody, M. C., Pye, H. O. T., Kelly, J. T., Lewandowski, M., Jaoui, M., Stevens, P. S., Brune, W. H., Lin, Y.-H., Rubitschun, C. L., and Surratt, J. D.: Gas and aerosol carbon in California: comparison of measurements and model predictions in Pasadena and Bakersfield, Atmos. Chem. Phys., 15, 5243-5258, doi:10.5194/acp-15-5243-2015, 2015.

Brown, S. G., Hyslop, N. P., Roberts, P. T., McCarthy, M. C., and Lurmann, F. W.: Wintertime vertical variations in particulate matter (PM) and precursor concentrations in the San Joaquin Valley during the California Regional Coarse PM/Fine PM Air Quality Study, J. Air Waste Manage., 56, 1267–1277, 2006.

Campbell, J. R., Tackett, J. L., Reid, J. S., Zhang, J., Curtis, C. A., Hyer, E. J., Sessions, W. R., Westphal, D. L., Prospero, J. M., Welton, E. J., Omar, A. H., Vaughan, M. A., and Winker, D. M.: Evaluating nighttime CALIOP 0.532 μm aerosol optical depth and extinction coefficient retrievals, Atmos. Meas. Tech., 5, 2143-2160, doi:10.5194/amtd-5-2143-2012, 2012.

Campbell., J. R., Ge, C., Wang, J., Welton, E. J., Bucholtz, A., Hyer, E. J., Reid, E. A., Chew, B. N., Liew, S.-C., Salinas, S. V., Lolli, S., Kaku, K. C., Lynch, P., Mahmud, M., Mohamad, M., and Holben, B. N.: Applying Advanced Ground-Based Remote Sensing in the Southeast Asian Maritime Continent to Characterize Regional Proficiencies in Smoke Transport Modeling, J. Appl. Meteorol. Climatol., 55, 3-22, doi: http://dx.doi.org/10.1175/JAMC-D-15-0083.1, 2016.

Chen, J., Lu, J., Avise, J. C., DaMassa, J. A., Kleeman, M. J., and Kaduwela, A. P.: Seasonal modeling of PM2.5 in California's San Joaquin Valley, Atmos. Environ., 92, 182–190, 2014.

Chow, J. C., Chen, L. W. A., Watson, J. G., Lowenthal, D. H., Magliano, K. A., Turkiewicz, K., Lehrman, D. E.: PM2.5 chemical composition and spatiotemporal variability during the

Atmos. Chem. Phys. Discuss., doi:10.5194/acp-2016-981, 2016
Manuscript under review for journal Atmos. Chem. Phys.
Published: 29 November 2016

California regional PM10/PM2.5 air quality study (CRPAQS), J. Geophys. Res.-Atmos., 111, D10S04, doi:10.1029/2005JD006457, 2006.

Dee, D. P., Uppala, S. M., Simmons, A. J., Berrisford, P., Poli, P, Kobayashi, S., Andrae, U., Balmaseda, M. A., Balsamo, G., Bauer, P., Bechtold, P., Beljaars, A. C. M., van de Berg, L., Bidlot, J., Bormann, N., Delsol, C., Dragani, R., Fuentes, M., Geer, A. J., Haimberger, L., Healy, S. B., Hersbach, H., Hólm, E. V., Isaksen, L., Kallberg, P., Köhler, M., Matricardi, M., McNally, A. P., Monge-Sanz, B. M., Morcrette, J.-J., Park, B.-K., Peubey, C., de Rosnay, P., Tavolato, C., Thépaut, J.-N., and Vitart, F.: The ERA-Interim reanalysis: configuration and performance of the data assimilation system, Q. J. R. Meteorol. Soc., 137, 553–597, 2011.

Diner, D. J., Beckert, J. C., Reilly, T. H., Bruegge, C. J., Conel, J. E., Kahn, R. A., Martonchik, J. V., Ackerman, T. P., Davies, R., Gerstl, S. A. W., Gordon, H. R., Muller, J. P., Myneni, R. B., Sellers, P. J., Pinty, B., and Verstraete, M. M.: Multi-angle Imaging SpectroRadiometer (MISR) Instrument Description and Experiment Overview, IEEE T. Geosci. Remote, 36, 1072–1087, 1998.

Divakarla, M. G., Barnet, C. D., Goldberg, M. D., McMillin, L. M., Maddy, E., Wolf, W., Zhou, L., and Liu, X.: Validation of Atmospheric Infrared Sounder temperature and water vapor retrievals with matched radiosonde measurements and forecasts, J. Geophys. Res., 111, D09S15, doi:10.1029/2005JD006116, 2006.

Eck, T. F., Holben, B. N., Reid, J. S., Dubovik, O., Smirnov, A., O'Neill, N. T., Slutsker, I., and Kinn, S.: Wavelength dependence of the optical depth of biomass burning urban, and desert dust aerosols, J. Geophys. Res., 104, 31333–31349, 1999.

Emmons, L. K., Walters, S., Hess, P. G., Lamarque, J.-F., Pfister, G. G., Fillmore, D., Granier, C., Guenther, A., Kinnison, D., Laepple, T., Orlando, J., Tie, X., Tyndall, G., Wiedinmyer, C., Baughcum, S. L., and Kloster, S.: Description and evaluation of the Model for Ozone and Related chemical Tracers, version 4 (MOZART-4), Geosci. Model Dev., 3, 43–67, doi: 10.5194/gmd-3-43-2010, 2010.

Fast, J. D., Gustafson Jr., W. I., Berg, L. K., Shaw, W. J., Pekour, M., Shrivastava, M., Barnard, J. C., Ferrare, R. A., Hostetler, C. A., Hair, J. A., Erickson, M., Jobson, B. T., Flowers, B., Dubey, M. K., Springston, S., Pierce, R. B., Dolislager, L., Pederson, J., and Zaveri, R. A.: Transport

Atmos. Chem. Phys. Discuss., doi:10.5194/acp-2016-981, 2016
Manuscript under review for journal Atmos. Chem. Phys.
Published: 29 November 2016

and mixing patterns over Central California during the carbonaceous aerosol and radiative effects study (CARES), Atmos. Chem. Phys., 12, 1759-1783, doi:10.5194/acp-12-1759-2012, 2012.

Fast, J. D., Allan, J., Bahreini, R., Craven, J., Emmons, L., Ferrare, R., Hayes, P. L., Hodzic, A., Holloway, J., Hostetler, C., Jimenez, J. L., Jonsson, H., Liu, S., Liu, Y., Metcalf, A., Middlebrook, A., Nowak, J., Pekour, M., Perring, A., Russell, L., Sedlacek, A., Seinfeld, J., Setyan, A., Shilling, J., Shrivastava, M., Springston, S., Song, C., Subramanian, R., Taylor, J. W., Vinoj, V., Yang, Q., Zaveri, R. A., and Zhang, Q.: Modeling regional aerosol and aerosol precursor variability over California and its sensitivity to emissions and long-range transport during the 2010 CalNex and CARES campaigns, Atmos. Chem. Phys., 14, 10013-10060, doi:10.5194/acp-14-10013-2014, 2014.

Fountoukis, C., Koraj, D., Denier van der Gon, H. A. C., Charalampidis, P. E., Pilinis, C., and Pandis, S. N.: Impact of grid resolution on the predicted fine PM by a regional 3-D chemical transport model, Atmos. Environ., 68, 24–32, 2013.

Ginoux, P., Chin, M., Tegen, I., Prospero, J. M., Holben, B., Dubovik, O., and Lin, S.: Sources and distributions of dust aerosols simulated with the GOCART model, J. Geophys. Res., 106, 20225–20273, 2001.

Gong, S. L.: A parameterization of sea-salt aerosol source function for sub- and super-micron particles, Global Biogeochem. Cy., 17, 1097, doi:10.1029/2003GB002079, 2003.

Grell, G. and Devenyi, D.: A generalized approach to parameterizing convection combining ensemble and data assimilation techniques, Geophys. Res. Lett., 29(14), doi:10.1029/2002GL015311, 2002.

Grell, G., Peckham, S., Schmitz, R., et al.: Fully coupled "online" chemistry within the WRF model, Atmos. Environ., 39(37), 6957–6975, 2005.

Guenther, A., Karl, T., Harley, P., Wiedinmyer, C., Palmer, P. I., and Geron, C.: Estimates of global terrestrial isoprene emissions using MEGAN (Model of Emissions of Gases and Aerosols from Nature), Atmos. Chem. Phys., 6, 3181–3210, doi: 10.5194/acp-6-3181-2006, 2006.

Atmos. Chem. Phys. Discuss., doi:10.5194/acp-2016-981, 2016
Manuscript under review for journal Atmos. Chem. Phys.
Published: 29 November 2016

473 Hand, J., Copeland, S. A., Day, D. E., Dillner, A. M., Indresand, H., Malm, W. C., McDade, C.
474 E., Moore Jr., C. T., Pitchford, M. L., Schichtel, B. A., and Watson, J. G.: Spatial and seasonal
475 patterns and temporal variability of haze and its constituents in the United States: Report V,
476 June 2011, available at: http://vista.cira.colostate.edu/Improve/spatial-and-seasonal-patterns-
477 and-temporal-variability-of-haze-and-its-constituents-in-the-united-states-report-v-june-
478 2011/, 2011.

479 Hasheminassab, S., Daher, N., Saffari, A., Wang, D., Ostro, B. D., and Sioutas, C.: Spatial and
480 temporal variability of sources of ambient fine particulate matter ($PM_{2.5}$) in California, Atmos.
481 Chem. Phys., 14, 12085-12097, doi:10.5194/acp-14-12085-2014, 2014.

482 Herner, J. D., Ying, Q., Aw, J., Gao, O., Chang, D. P. Y., and Kleeman, M.: Dominant mechanisms
483 that shape the airborne particle size and composition in central California, Aerosol Sci.
484 Technol., 40, 827–844, 2006.

485 Holben, B. N., Eck, T. F., Slutsker, I., Tanre ì, D., Buis, J. P., Setzer, A., Vermote, E., Reagan, J.
486 A., Kaufman, Y. J., Nakajima, T., Lavenu, F., Jankowiak, I., and Smirnov, A.: AERONET –
487 A Federated Instrument Network and Data Archive for Aerosol Characterization, Remote
488 Sens. Environ., 66, 1–16, 1998.

489 Holben, B. N., Tanr, D., Smirnov, A., Eck, T. F., Slutsker, I., Abuhassan, N., Newcomb, W. W.,
490 Schafer, J. S., Chatenet, B., Lavenu, F., Kaufman, Y. J., Castle, J. V., Setzer, A., Markham,
491 B., Clark, D., Frouin, R., Halthore, R., Karneli, A., O'Neill, N. T., Pietras, C., Pinker, R. T.,
492 Voss, K., and Zibordi, G.: An emerging ground-based aerosol climatology: Aerosol optical
493 depth from AERONET, J. Geophys. Res., 106, 12067–12097, 2001.

494 Hong, S., Noh, Y., and Dudhia, J.: A new vertical diffusion package with an explicit treatment of
495 entrainment processes, Mon. Weather Rev., 134, 2318–2341, 2006.

496 Hu, Z., Zhao, C., Huang, J., Leung, L. R., Qian, Y., Yu, H., Huang, L., and Kalashnikova, O. V.:
497 Trans-Pacific transport and evolution of aerosols: evaluation of quasi-global WRF-Chem
498 simulation with multiple observations, Geosci. Model Dev., 9, 1725-1746, doi:10.5194/gmd-
499 9-1725-2016, 2016.

Atmos. Chem. Phys. Discuss., doi:10.5194/acp-2016-981, 2016
Manuscript under review for journal Atmos. Chem. Phys.
Published: 29 November 2016

500 Iacono, M. J., Delamere, J. S., Mlawer, E. J., Shephard, M. W., Clough, S. A., and Collins, W. D.:
501 Radiative forcing by long-lived greenhouse gases: calculations with the AER radiative transfer
502 models, J. Geophys. Res., 113, D13103, doi:10.1029/2008JD009944, 2008.

503 Jaeglé, L., Quinn, P. K., Bates, T. S., Alexander, B., and Lin, J.-T.: Global distribution of sea salt
504 aerosols: new constraints from in situ and remote sensing observations, Atmos. Chem. Phys.,
505 11, 3137–3157, doi:10.5194/acp-11-3137-2011, 2011.

506 Kahn, R. A., Gaitley, B. J., Garay, M. J., Diner, D. J., Eck, T. F., Smirnov, A., and Holben, B. N.:
507 Multiangle Imaging SpectroRadiometer global aerosol product assessment by comparison with
508 the Aerosol Robotic Network, J. Geophys. Res., 115, D23209, doi:10.1029/2010JD014601,
509 2010.

510 Kassianov, E., Pekour, M., and Barnard, J.: Aerosols in central California: Unexpectedly large
511 contribution of coarse mode to aerosol radiative forcing, Geophys. Res. Lett., 39, L20806, doi:
512 10.1029/2012GL053469, 2012.

513 Kelly, J. T., Baker, K. R., Nowak, J. B., Murphy, J. G., Markovic, M. Z., VandenBoer, T. C., Ellis,
514 R. A., Neuman, J. A., Weber, R. J., and Roberts, J. M.: Fine-scale simulation of ammonium
515 and nitrate over the South Coast Air Basin and San Joaquin Valley of California during
516 CalNex-2010, J. Geophys. Res.-Atmos., 119, 3600–3614, 2014.

517 Kim, S.-W., McKeen, S. A., Frost, G. J., Lee, S.-H., Trainer, M., Richter, A., Angevine, W. M.,
518 Atlas, E., Bianco, L., Boersma, K. F., Brioude, J., Burrows, J. P., de Gouw, J., Fried, A.,
519 Gleason, J., Hilboll, A., Mellqvist, J., Peischl, J., Richter, D., Rivera, C., Ryerson, T., te Lintel
520 Hekkert, S., Walega, J., Warneke, C., Weibring, P., and Williams, E.: Evaluations of NO_x and
521 highly reactive VOC emission inventories in Texas and their implications for ozone plume
522 simulations during the Texas Air Quality Study 2006, Atmos. Chem. Phys., 11, 11361-11386,
523 doi:10.5194/acp-11-11361-2011, 2011.

524 Lawrence, D. M., Oleson, K. W., Flanner, M. G., Thornton, P. E., Swenson, S. C., Lawrence, P.
525 J., Zeng, X., Yang, Z.-L., Levis, S., Sakaguchi, K., Bonan, G. B., and Slater, A. G.:
526 Parameterization improvements and functional and structural advances in version 4 of the
527 Community Land Model, J. Adv. Model. Earth Sys., 3, M03001, doi:
528 10.1029/2011MS000045, 2011.

Atmos. Chem. Phys. Discuss., doi:10.5194/acp-2016-981, 2016
Manuscript under review for journal Atmos. Chem. Phys.
Published: 29 November 2016

529 Misenis, C. and Zhang, Y.: An examination of sensitivity of WRF/Chem predictions to physical
530 parameterizations, horizontal grid spacing, and nesting options, Atmos. Res., 97, 315–334,
531 doi:10.1016/j.atmosres.2010.04.005, 2010.

532 Morabito, D., Wu, L., and Slobin, S.: Weather Forecasting for Ka-band Operations: Initial Study
533 Results, IPN PR 42-206, pp. 1-24, August 15, 2016. Available at:
534 http://ipnpr.jpl.nasa.gov/progress_report/42-206/206C.pdf, 2016.

535 Morrison, H., Thompson, G., and Tatarskii, V.: Impact of cloud microphysics on the development
536 of trailing stratiform precipitation in a simulated squall line: comparison of one- and two-
537 moment schemes, Mon. Weather Rev., 137, 991–1007, 2009.

538 Omar, A.H., Winker, D.M., Kittaka, C., Vaughan, M.A., Liu, Z., Hu, Y., Trepte, C.R., Rogers,
539 R.R., Ferrare, R.A., Lee, K.P., Kuehn, R.E., Hostetler, C.A.: The CALIPSO automated aerosol
540 classification and lidar ratio selection algorithm. J. Atmos. Ocean. Technol. 26, 1994–2014,
541 2009.

542 Pun, B. K., Balmori, R. T. F., and Seigneur, C.: Modeling wintertime particulate matter formation
543 in central California, Atmos. Environ., 43, 402–409, 2009.

544 Qian, Y., Gustafson Jr., W. I., and Fast, J. D.: An investigation of the sub-grid variability of trace
545 gases and aerosols for global climate modeling, Atmos. Chem. Phys., 10, 6917-6946,
546 doi:10.5194/acp-10-6917-2010, 2010.

547 Randerson, J. T., van der Werf, G. R., Giglio, L., Collatz, G. J., and Kasibhatla, P. S.: Global Fire
548 Emissions Database, Version 2 (GFEDv2.1). Data set. Available on-line [http://daac.ornl.gov/]
549 from Oak Ridge National Laboratory Distributed Active Archive Center, Oak Ridge,
550 Tennessee, U.S.A. doi:10.3334/ORNLDAAC/849, 2007.

551 San Joaquin Valley Air Pollution Control District: 2012 PM2.5 plan. Available from:
552 http://www.valleyair.org/Air_Quality_Plans/PM25Plans2012.htm, 2012.

553 Scarino, A. J., Obland, M. D., Fast, J. D., Burton, S. P., Ferrare, R. A., Hostetler, C. A., Berg, L.
554 K., Lefer, B., Haman, C., Hair, J. W., Rogers, R. R., Butler, C., Cook, A. L., and Harper, D.
555 B.: Comparison of mixed layer heights from airborne high spectral resolution lidar, ground-
556 based measurements, and the WRF-Chem model during CalNex and CARES, Atmos. Chem.
557 Phys., 14, 5547-5560, doi:10.5194/acp-14-5547-2014, 2014.

Atmos. Chem. Phys. Discuss., doi:10.5194/acp-2016-981, 2016
Manuscript under review for journal Atmos. Chem. Phys.
Published: 29 November 2016

558 Shaw, W., Allwine, K. J., Fritz, B. G., Rutz, F. C., Rishel, J. P., and Chapman, E. G.: An evaluation
559 of the wind erosion module in DUSTRAN, Atmos. Environ., 42, 1907–1921, 2008.

560 Solomon, P. A., Crumpler, D., Flanagan, J. B., Jayanty, R. K. M., Rickman, E. E., and McDade C.
561 E.: U.S. National PM 2.5 Chemical Speciation Monitoring Networks – CSN and IMPROVE:
562 Description of Networks, J. Air Waste Manage., 64, 1410–1438,
563 doi:10.1080/10962247.2014.956904, 2014.

564 Susskind, J., Barnet, C. D., and Blaisdell, J.: Retrieval of atmospheric and surface parameters from
565 AIRS/AMSU/HSB data under cloudy conditions, IEEE Trans. Geosci. Remote Sens., 41(2),
566 390–409, doi:10.1109/TGRS.2002.808236, 2003.

567 Tessum, C. W., Hill, J. D., and Marshall, J. D.: Twelve-month, 12 km resolution North American
568 WRF-Chem v3.4 air quality simulation: performance evaluation, Geosci. Model Dev., 8, 957-
569 973, doi:10.5194/gmd-8-957-2015, 2015.

570 Toth, T. D., Campbell, J. R., Reid, J. S., Tackett, J. L., Vaughan, M. A. and Zhang, J.: Lower
571 daytime threshold sensitivities to aerosol optical thickness in CALIPSO Level 2 products, J.
572 Atmos. Oceanic. Technol., in review, 2016.

573 US Environmental Protection Agency, 2010: Technical Support Document: Preparation of
574 Emissions Inventories for the Version 4, 2005-based Platform, 73 pp., Office of Air Quality
575 Planning and Standards, Air Quality Assessment Division, available at:
576 https://www3.epa.gov/crossstaterule/pdfs/2005_emissions_tsd_07jul2010.pdf, 2010.

577 Wu, L., and Petty, G. W. : Intercomparison of Bulk Microphysics Schemes in Simulations of Polar
578 lows. Mon. Wea. Rev., 138, 2211-2228. doi: 10.1175/2010MWR3122.1, 2010.

579 Wu, L., Su, H. and Jiang, J. H.: Regional simulations of deep convection and biomass burning
580 over South America: 1. Model evaluations using multiple satellite data sets, J. Geophys. Res.,
581 116, D17208, doi:10.1029/2011JD016105, 2011a.

582 Wu, L., Su, H. and Jiang, J. H.: Regional simulations of deep convection and biomass burning
583 over South America: 2. Biomass burning aerosol effects on clouds and precipitation, J.
584 Geophys. Res., 116, D17209, doi:10.1029/2011JD016106, 2011b.

Atmos. Chem. Phys. Discuss., doi:10.5194/acp-2016-981, 2016
Manuscript under review for journal Atmos. Chem. Phys.
Published: 29 November 2016

585 Wu, L., Su, H. and Jiang, J. H.: Regional simulations of aerosol impacts on precipitation during
586 the East Asian summer monsoon. J. Geophys. Res. Atmos., 118, doi: 10.1002/jgrd.50527,
587 2013.

588 Wu, L., Li, J.-L. F., Pi, C.-J., Yu, J.-Y., and Chen, J.-P.: An observationally based evaluation of
589 WRF seasonal simulations over the Central and Eastern Pacific, J. Geophys. Res. Atmos., 120,
590 doi:10.1002/2015JD023561, 2015.

591 Ying, Q. and Kleeman, M. J.: Regional contributions to airborne particulate matter in central
592 California during a severe pollution episode, Atmos. Environ., 43, 1218–1228, 2009.

593 Young, S.A. and Vaughan, M.A.: The retrieval of profiles of particulate extinction from Cloud–
594 Aerosol Lidar Infrared Pathfinder Satellite Observations (CALIPSO) data: algorithm
595 description. J. Atmos. Ocean. Technol. 26, 1105–1119, 2009.

596 Zhang, Y., Liu, P., Liu, X.-H., Pun, B., Seigneur, C., Jacobson, M. Z., and Wang, W.-X.: Fine
597 scale modeling of wintertime aerosol mass, number, and size distributions in central California,
598 J. Geophys. Res.-Atmos., 115, D15207, doi:10.1029/2009jd012950, 2010.

599 Zhao, C., Liu, X., Leung, L. R., Johnson, B., McFarlane, S. A., Gustafson Jr., W. I., Fast, J. D.,
600 and Easter, R.: The spatial distribution of mineral dust and its shortwave radiative forcing over
601 North Africa: modeling sensitivities to dust emissions and aerosol size treatments, Atmos.
602 Chem. Phys., 10, 8821–8838, doi: 10.5194/acp-10-8821-2010, 2010.

603 Zhao, C., Leung, L. R., Easter, R., Hand, J., and Avise, J.: Characterization of speciated aerosol
604 direct radiative forcing over California, J. Geophys. Res., 118, 2372–2388, doi:
605 10.1029/2012JD018364, 2013.

606 Zhao, C., Hu, Z., Qian, Y., Ruby Leung, L., Huang, J., Huang, M., Jin, J., Flanner, M. G., Zhang,
607 R., Wang, H., Yan, H., Lu, Z., and Streets, D. G.: Simulating black carbon and dust and their
608 radiative forcing in seasonal snow: a case study over North China with field campaign
609 measurements, Atmos. Chem. Phys., 14, 11475-11491, doi:10.5194/acp-14-11475-2014,
610 2014.

Atmos. Chem. Phys. Discuss., doi:10.5194/acp-2016-981, 2016
Manuscript under review for journal Atmos. Chem. Phys.
Published: 29 November 2016

List of Table

Table 1. Experiment description

Experiment ID	Experiment description
20km	Simulation with the GOCART dust scheme at 20 km horizontal resolution.
4km	Same as 20km, but at 4 km horizontal resolution.
4km_D2	Same as 4km, but with the DUSTRAN dust scheme.

Atmos. Chem. Phys. Discuss., doi:10.5194/acp-2016-981, 2016
Manuscript under review for journal Atmos. Chem. Phys.
Published: 29 November 2016

614 Table 2. Surface aerosol mass (μg m^{-3}) for different species at Fresno, CA

Species	Cold season				Warm season			
	IMPROVE	20km	4km	4km_D2	IMPROVE	20km	4km	4km_D2
PM2.5	16.84	13.71	21.38	22.48	8.44	4.91	6.29	12.85
PM2.5_NO_3	5.43	6.36	9.54	9.22	0.84	0.55	0.69	0.79
PM2.5_OC	3.85	0.92	2.07	2.07	1.76	0.49	0.87	0.87
PM2.5_EC	1.08	0.52	1.12	1.13	0.32	0.27	0.49	0.49
PM2.5_SO_4	0.87	0.53	0.82	0.81	1.04	0.54	0.61	0.60
PM2.5_dust	0.90	0.11	0.11	1.65	2.08	0.04	0.03	6.49
PM10	31.55	14.93	22.81	28.32	34.82	7.08	8.69	38.12

615

Atmos. Chem. Phys. Discuss., doi:10.5194/acp-2016-981, 2016
Manuscript under review for journal Atmos. Chem. Phys.
Published: 29 November 2016

List of Figures

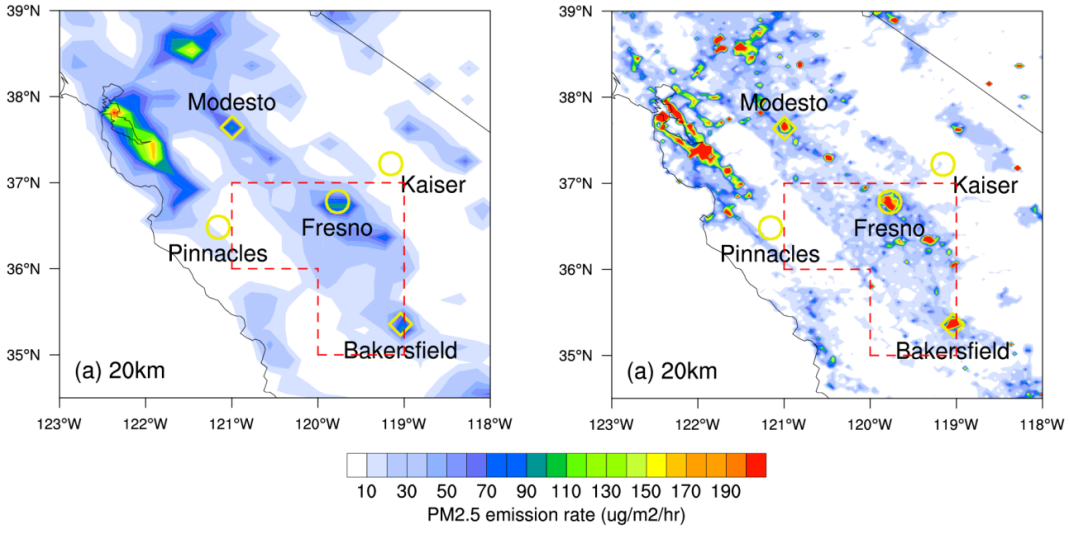

Figure 1. Daily mean anthropogenic PM2.5 emission rate (μg m^{-2} s^{-1}) at (a) 20km and (b) 4km simulation. Red dashed lines in Figure 1a represent the region used for domain averages in Figure 8 and 9. Yellow circle: IMPROVE site; yellow diamond: EPA CSN site. Three urban sites: Fresno, Bakersfield and Modesto; two rural sites: Pinnacles and Kaiser.

Atmos. Chem. Phys. Discuss., doi:10.5194/acp-2016-981, 2016
Manuscript under review for journal Atmos. Chem. Phys.
Published: 29 November 2016

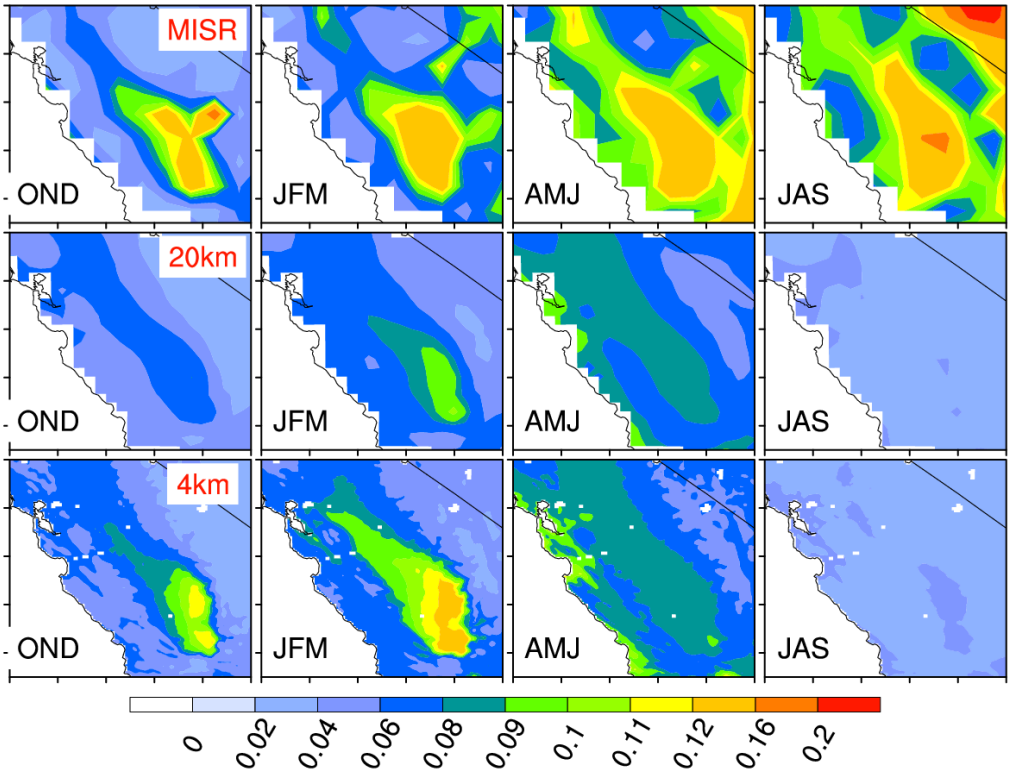

622

623 Figure 2. Spatial distribution of seasonal mean 550 nm AOD from MISR and the WRF-Chem
624 (20km and 4km) simulations in WY2013. OND: October, November and December; JFM: January,
625 February and March; AMJ: April, May and June; JAS: July, August and September.

Atmos. Chem. Phys. Discuss., doi:10.5194/acp-2016-981, 2016
Manuscript under review for journal Atmos. Chem. Phys.
Published: 29 November 2016

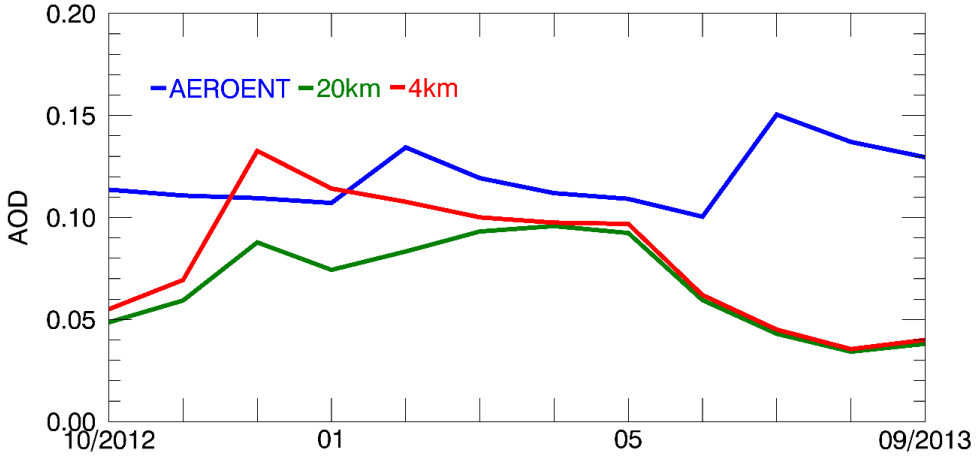

626

627 Figure 3. Monthly mean 550 nm AOD at Fresno, CA from October 2012 to September 2013.

Atmos. Chem. Phys. Discuss., doi:10.5194/acp-2016-981, 2016
Manuscript under review for journal Atmos. Chem. Phys.
Published: 29 November 2016

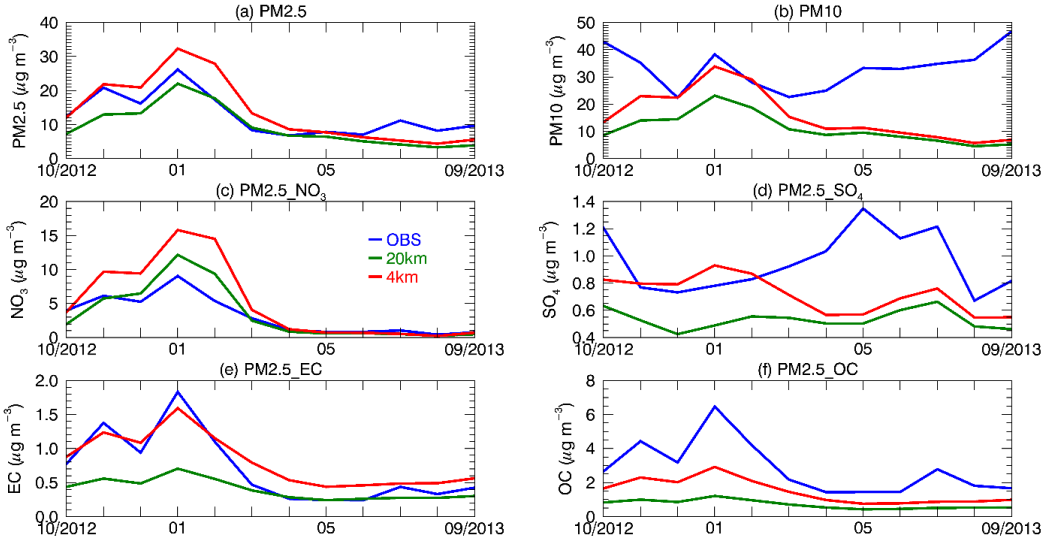

628

629 Figure 4. Aerosol mass (μg m^{-3}) for different species from IMPROVE (OBS), 20km and 4km
630 simulations at Fresno, CA. PM2.5_NO_3 represents NO_3 with diameter ≤2.5 μm. Similar definition
631 for SO_4, EC and OC in the figures.

Atmos. Chem. Phys. Discuss., doi:10.5194/acp-2016-981, 2016
Manuscript under review for journal Atmos. Chem. Phys.
Published: 29 November 2016

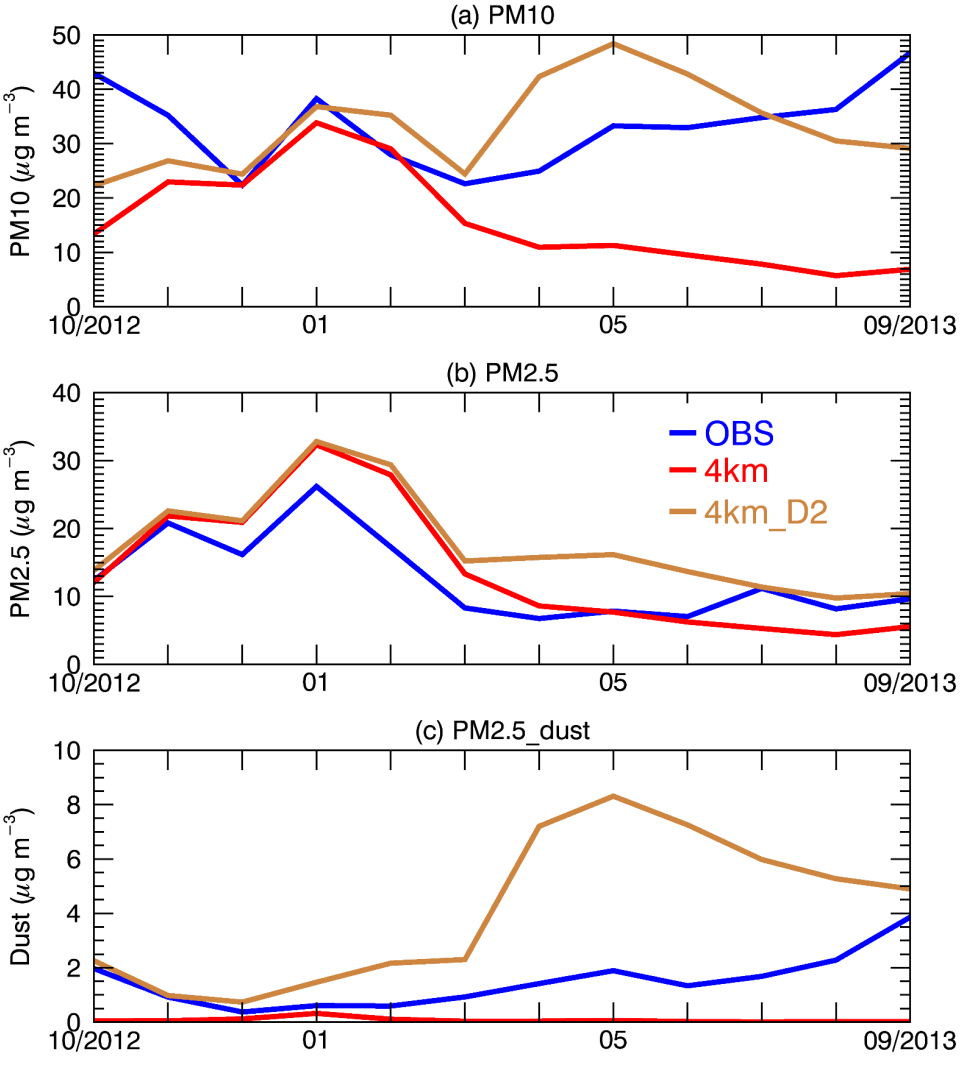

632

633 Figure 5. (a) PM10; (b) PM2.5; (c) PM2.5_dust from IMPROVE (OBS), 4km and 4km_D2
634 simulations at Fresno, CA.

Atmos. Chem. Phys. Discuss., doi:10.5194/acp-2016-981, 2016
Manuscript under review for journal Atmos. Chem. Phys.
Published: 29 November 2016

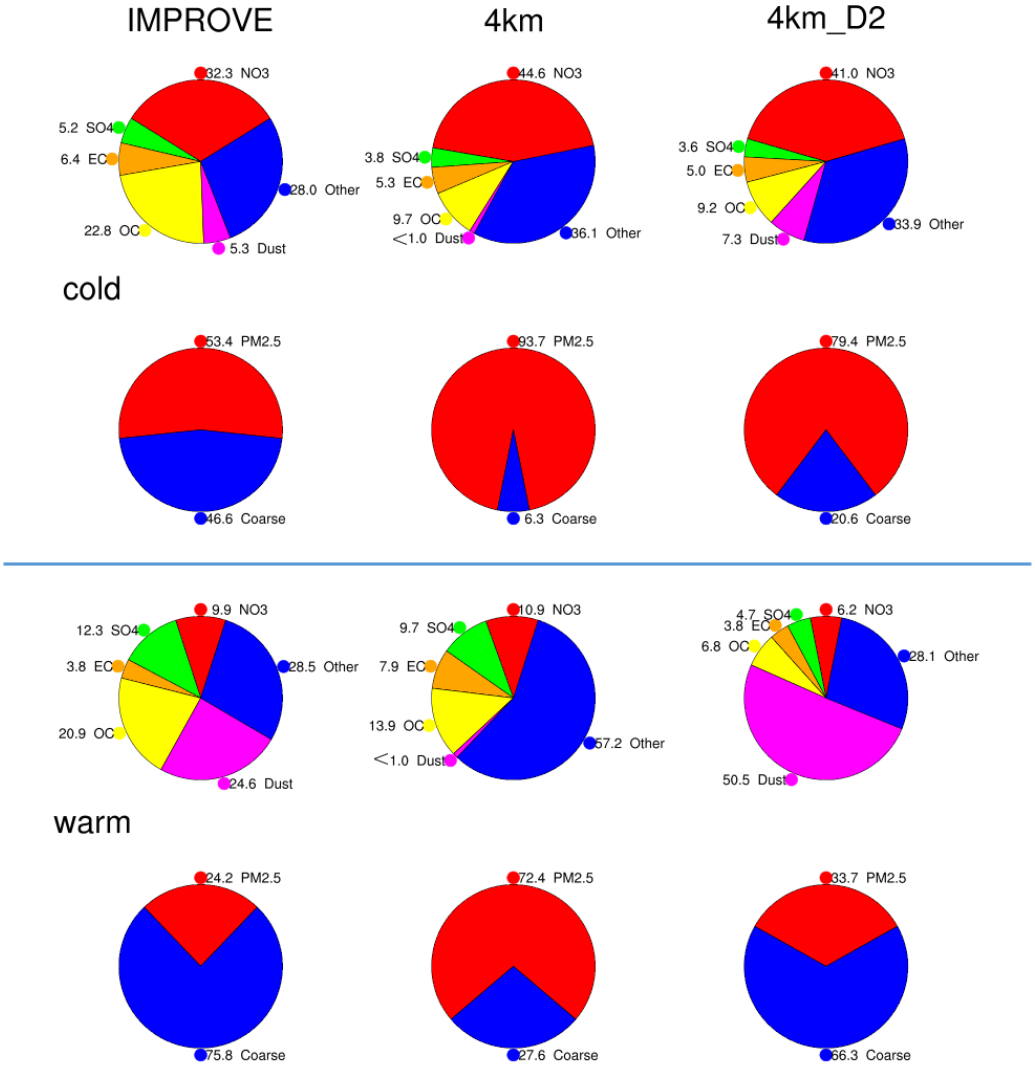

635

636 Figure 6. Relative contribution (%) of aerosol species from IMPROVE and the WRF-Chem
637 simulations (4km and 4km_D2) at Fresno, CA in WY2013. (Panel 1) Contribution to PM2.5 in
638 cold season; (Panel 2) relative contribution of PM2.5 and coarse mass to PM10 in cold season;
639 (Panel 3) same as Panel 1 but in warm season; (Panel 4) same as Panel 2 but in warm season.

Atmos. Chem. Phys. Discuss., doi:10.5194/acp-2016-981, 2016
Manuscript under review for journal Atmos. Chem. Phys.
Published: 29 November 2016

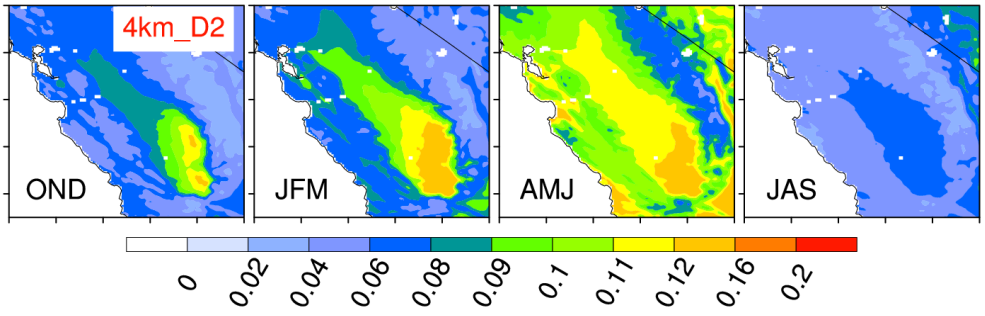

640

641 Figure 7. Spatial distribution of seasonal mean 550 nm AOD from 4km_D2 in WY2013.

Atmos. Chem. Phys. Discuss., doi:10.5194/acp-2016-981, 2016
Manuscript under review for journal Atmos. Chem. Phys.
Published: 29 November 2016

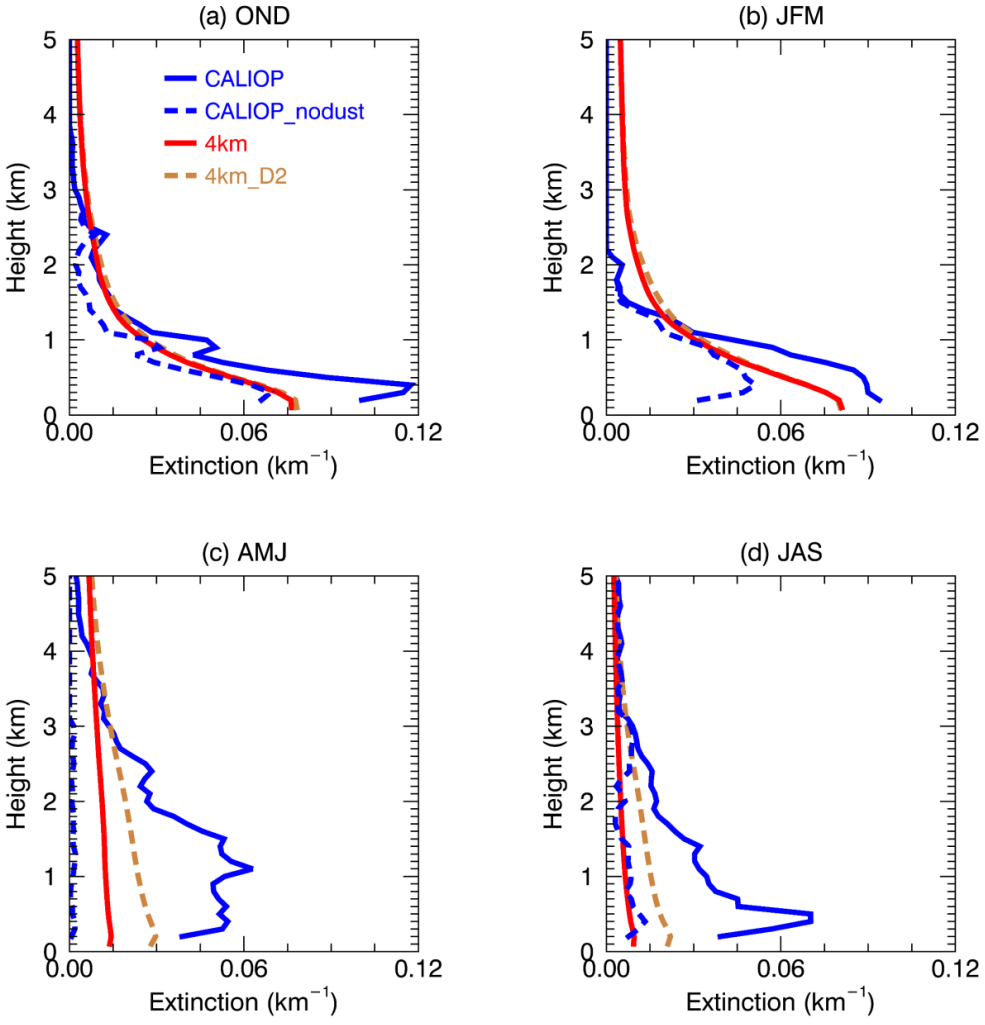

642

643 Figure 8. Vertical distribution of seasonal mean 532 nm aerosol extinction coefficient (km^{-1})
644 from CALIOP (blue) and the WRF-Chem (4km and 4km_D2) simulations over the red box
645 region in Figure 1a) in WY2013. Blue dashed lines (CALIOP_nodust) represent the CALIOP
646 profiles without dust (dust and polluted dust).

Atmos. Chem. Phys. Discuss., doi:10.5194/acp-2016-981, 2016
Manuscript under review for journal Atmos. Chem. Phys.
Published: 29 November 2016

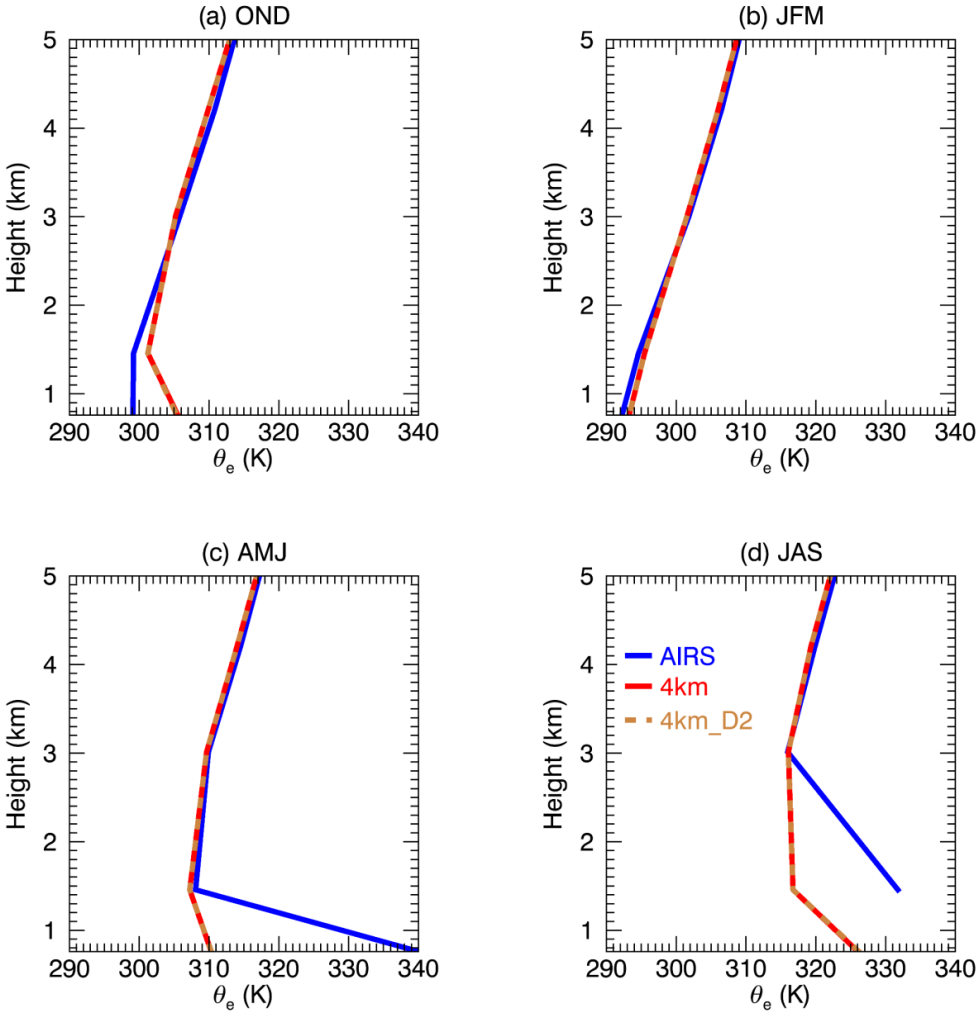

647

648 Figure 9. Vertical distribution of season mean equivalent potential temperature (θ_e; K) from AIRS
649 and the WRF-Chem (4km and 4km_D2) simulations over the red box region in Figure 1a in
650 WY2013.

Atmos. Chem. Phys. Discuss., doi:10.5194/acp-2016-981, 2016
Manuscript under review for journal Atmos. Chem. Phys.
Published: 29 November 2016

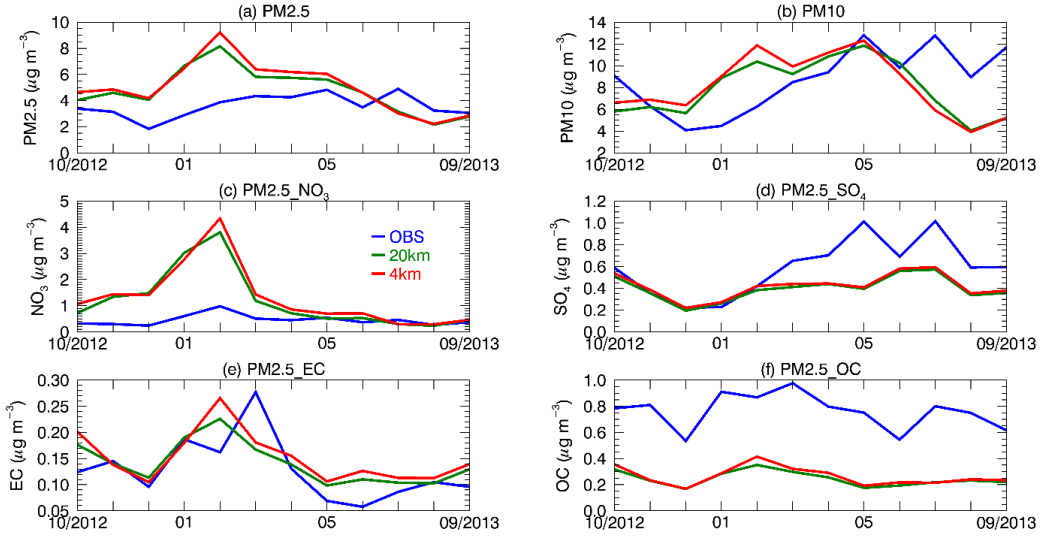

Figure 10. Aerosol mass (μg m^{-3}) for different species from IMPROVE (OBS), 20km and 4km simulations at Pinnacles, CA.

Atmos. Chem. Phys. Discuss., doi:10.5194/acp-2016-981, 2016
Manuscript under review for journal Atmos. Chem. Phys.
Published: 29 November 2016

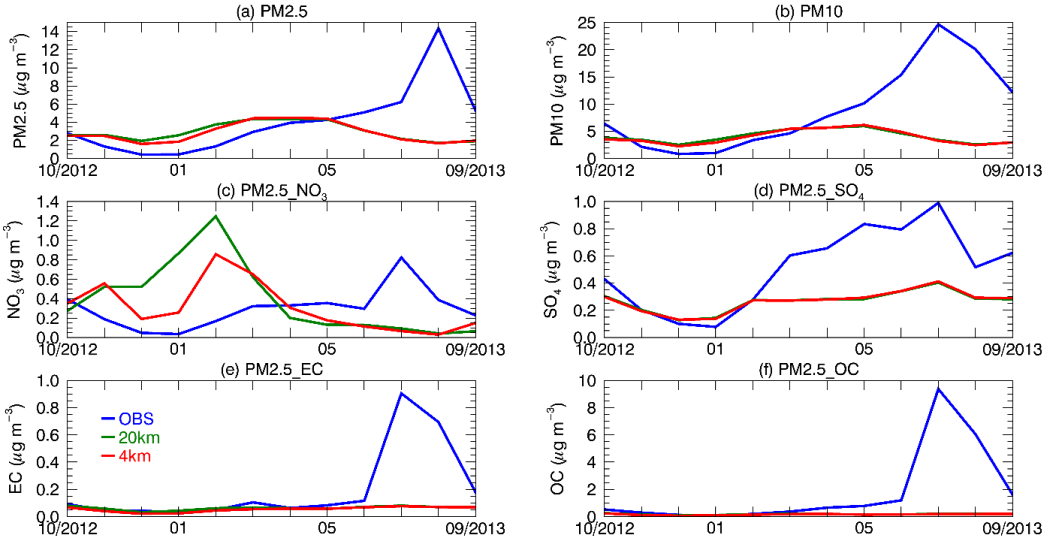

654

655 Figure 11. Aerosol mass (μg m^{-3}) for different species from IMPROVE (OBS), 20km and 4km
656 simulations at Kaiser, CA.